

Received August 10, 2020, accepted August 13, 2020, date of publication August 17, 2020, date of current version August 28, 2020.

Digital Object Identifier 10.1109/ACCESS.2020.3017236

Three-Point Marking Method to Overcome External Parameter Disturbance in Stereo-DIC Based on Camera Pose Self-Estimation

CHANG MA^{ID}, ZHOUMO ZENG^{ID}, (Member, IEEE), HUI ZHANG^{ID}, (Member, IEEE), HENGRUI CUI^{ID}, AND XIAOBO RUI^{ID}

State Key Laboratory of Precision Measuring Technology and Instruments, Tianjin University, Tianjin 300072, China

Corresponding author: Zhoumo Zeng (zhmzeng@tju.edu.cn)

This work was supported by the National Key Research and Development Program of China under Grant 2016YFF0101802.

ABSTRACT Stereo digital image correlation (stereo-DIC) requires the stereo-camera system to remain fixed during the measurement process. This requirement brings a lot of inconvenience to the practical application of stereo-DIC. In many application scenarios such as dynamic measurement, the external parameters of the camera are almost inevitably disturbed, which will bring great errors to the DIC measurement results. To overcome this problem, this paper proposes a three-point marking method to determine the world coordinate system and a camera pose self-estimation method based on speckle patterns. The three-point marking method can use three undeformed feature points in the field of view (FOV) to determine the world coordinate system. The proposed camera pose self-estimation method can calculate the pose parameters of the binocular camera at the shooting time of each frame of image. This method does not require plane assumptions and has good applicability. Simulations and experiments were carried out to verify the effectiveness of the proposed scheme in overcoming external parameter disturbances.

INDEX TERMS Stereo digital image correlation, external parameter disturbance, self-calibration, camera pose self-estimation.

I. INTRODUCTION

Digital image correlation (DIC) is an optical measurement method that measures the displacement and strain fields of an object due to deformation. It has the advantages of full-field measurement, simple equipment, and low environment requirements [1]–[3]. DIC is mainly used in the field of optical measurement mechanics, but it has applications in many fields such as structural health monitoring, non-destructive testing, biological testing, and vibration measurement [4]–[9]. The stereo digital image correlation (stereo-DIC) measurement generally relies on a stereo-camera system except for a small number of cases where a single camera is used to realize three-dimensional measurement with a plane mirror [10]. Before the stereo-DIC measurement starts, the stereo-camera system needs to be calibrated. Almost all calculations in stereo-DIC rely on camera parameters obtained by calibration. The parameters obtained by calibration can be divided into internal parameters and

external parameters. Internal parameters refer to the camera's focal length, principal point, and lens distortion coefficient. The external parameters refer to the pose of the camera. The pose parameters of the stereo-camera system are generally expressed by the rotation and translation of the right camera relative to the left camera. The accuracy of the calibration results greatly affects the accuracy of the stereo-DIC measurement results. Therefore, DIC requires that the internal and external parameters of the stereo-camera system cannot be changed during the entire measurement process. The cameras used must not have any rotation or movement. This requirement greatly limits the application of DIC and brings a lot of inconvenience to researchers in practical applications. For example, when performing dynamic measurements or vibration measurements, it is almost impossible for the external parameters of the camera not to be disturbed [11], [12]. When the camera needs to be placed at an angle, the camera may rotate or slip due to the influence of gravity. When taking measurements outdoors, it is often difficult to ensure that cameras are not disturbed. Once the external parameters of the camera are disturbed, it will cause great errors in the

The associate editor coordinating the review of this manuscript and approving it for publication was Yizhang Jiang^{ID}.

measurement results, and even the data obtained during the entire measurement process will become unavailable, which will cause a lot of waste. If the restriction that the camera pose cannot be changed is lifted, stereo-DIC technology will become more flexible. The application of stereo-DIC technology under non-laboratory conditions, such as structural health monitoring, will be further expanded.

At present, there are few researches on the problem of camera pose disturbance in stereo-DIC. Recently, Su *et al.* [13] proposed a real-time external parameter correction method for stereo-DIC to overcome the predicament of reduced measurement accuracy due to the unavoidable disturbance of external parameters. To the best of our knowledge, this is the first time that a method for real-time correction of external parameters has been proposed. They proposed an automatic calibration method based on the speckle pattern on the surface of the measured object, which effectively overcome the limitations of the traditional calibration method. They adopted a real-time optimization method to reduce the impact of external parameter disturbances on measurement accuracy. However, they did not discuss the problem of resetting the world coordinate system and did not fundamentally eliminate the effect of external parameter disturbance on stereo-DIC.

To overcome the impact of external parameter disturbance on stereo-DIC, two problems need to be solved. First, there must be a fixed reference as the world coordinate system. Second, it is necessary to be able to calculate the camera pose in real time. There are generally three ways to set the world coordinate system. One is to use the left camera coordinate system as the world coordinate system. The second is to set the world coordinate system with the calibration board as a reference during the calibration of the stereo-camera system [14]. The third is to set the world coordinate system with the surface of the measured object at the initial time as a reference [15]. The advantage of using the left camera coordinate system as the world coordinate system is that the calculation is simple. The external parameters obtained by calibration are directly used for calculation, and no additional coordinate conversion is required. The advantage of setting the world coordinate system with the surface of the measured object at the initial time as a reference is that the calculated results can more directly reflect the deformation of the measured object. However, all the above three ways require the camera to be stationary. Even if the position of the measured object at initial time is used as the world coordinate system, the camera still needs to be fixed so that the three dimensional reconstruction results at other times can be correctly converted into the world coordinate system. For the second problem, the real-time calculation of camera pose is a kind of self-calibration method. Whether in the field of computer vision or in the DIC community, the self-calibration method is a topic that has received widespread attention. Liu *et al.* [16] proposed a self-calibration method for stereo cameras based on SIFT. They used the epipolar geometry relationship between the two views of the binocular camera to solve the camera pose parameters. Chen and Pan [17] proposed a

camera calibration method based on speckle patterns, proving that speckle patterns in DIC technology can also be used for calibration. Shao *et al.* [18] designed a self-calibration single camera 3D-DIC system. First, they used the constraint that the corresponding points in the binocular view should be in the polar plane to construct an optimization algorithm to solve for external parameters. Then roughly estimate the internal parameters according to the hardware parameters of the cameras. Finally, using the reprojection error as the cost function, a global optimization framework is constructed to solve all the internal and external parameters. Their method is very enlightening and groundbreaking, but this method relies on reliable initial values and requires that the internal parameters of the left and right cameras be the same.

This paper proposes a three-point marking method for setting the world coordinate system and a camera pose self-estimation method based on speckle patterns. In the usual DIC technology, the stereo-camera system not only undertakes the function of acquiring images, but also the important function of positioning. This is the fundamental reason why the external parameter disturbance easily affects the DIC measurement. The proposed three-point marking method makes the cameras no longer assume the positioning function. Its use requirement is that there are three non-collinear feature points in the view that have not moved during the measurement process. The three feature points assume the positioning function. These three feature points can be marked on a specially set marking object, on the holding device of the measured object, or on the part where the measured object itself has not been deformed. It is more stable to keep a small area marked with three feature points stationary than to keep a stereo-camera system stationary. Because the stereo-camera system is usually set on a tripod that is not bolted to the ground, and the camera often needs to adjust the angle of view. In addition to the problem of setting the world coordinate system, to overcome the disturbance of the external parameters of the camera, it is also necessary to make the DIC have the function of camera pose self-estimation. Therefore, this paper also proposes a self-estimation method of camera pose based on speckle pattern. Correlation calculations in DIC technology can obtain a large number of corresponding points in the binocular view. The epipolar geometric relations of these corresponding points are used to solve the external parameters, and the obtained external parameters are used as initial values. Then, the bundle adjustment (BA) method is used to solve the optimal solution of the external parameters. The proposed method only needs a pair of images of binocular view, and there is no plane assumption, that is, the surface of the object to be measured does not need to be flat. Therefore, it has strong applicability and can provide stable and reliable external parameters. To our knowledge, this is the first time that a complete solution to the problem of external parameter disturbance has been proposed.

The remainder of this paper is organized as follows. In the Section 2, the principle of the camera pose self-estimation method based on speckle pattern and the three-point marking

method are described. A complete stereo-DIC algorithm framework integrating these two functions is also shown. In Section 3, the effectiveness of the three-point marking method and the camera pose self-estimation method is verified through simulation. In Section 4, two experiments were carried out to verify the effectiveness of the proposed methods. In the experiment, the stereo-camera system was violently disturbed artificially. The proposed scheme effectively overcomes the influence of the camera disturbance. Section 5 is the conclusion.

II. PRINCIPLE

A. SELF-ESTIMATION METHOD OF CAMERA POSE BASED ON SPECKLE PATTERN

Stereo-DIC generally uses two cameras to form a stereo-camera system. The inherent projective geometric relationship between the left and right views of the binocular camera is epipolar geometry [19]. The epipolar geometry can be expressed by fundamental matrix:

$$q_2^T F q_1 = 0, \quad (1)$$

where q_1 and q_2 are the coordinates of the corresponding points in the left and right images of the binocular camera, and F is the fundamental matrix. After obtaining the internal parameters of the left and right cameras, the essential matrix can be calculated from the fundamental matrix:

$$E = K_2^T F K_1, \quad (2)$$

where K_1 and K_2 are the internal parameter matrices of the left and right cameras respectively, and E is the essential matrix. The essential matrix contains information about the rotation and translation between the left and right cameras. It connects the pose relationship between the two cameras through points in space:

$$E = [t]_{\times} R, \quad (3)$$

where R and t represent the rotation matrix and translation vector between the left and right cameras, respectively. R and t can be obtained by singular value decomposition (SVD) of the essential matrix.

To calculate the essential matrix, the corresponding points in the left and right images of the stereo-camera system are required. Correlation operations in DIC technology can obtain thousands of corresponding points between left and right images. After the cameras' internal parameters are obtained through calibration, the essential matrix can be calculated. A five-point algorithm based on the Random Sample Consensus (RANSAC) framework was used to calculate a reliable essential matrix through the corresponding points [20], [21]. By decomposing the essential matrix, the initial value estimate of the camera pose can be obtained. After that, the bundle adjustment (BA) method is used to optimize the camera pose parameters. The schematic diagram of the BA method is shown in Figure 1. Assuming that there are n pairs of corresponding points participating in BA optimization, let q_{ij} be the pixel coordinates of the i -th point in image j . j is 1 for the left image and j is 2 for the right image.

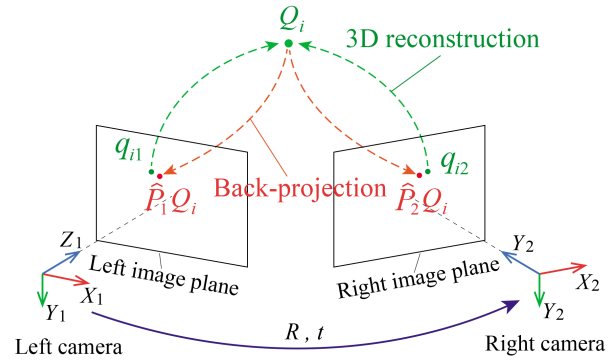


FIGURE 1. Schematic diagram of bundle adjustment method.

Three-dimensional (3D) reconstruction is performed in the left camera coordinate system, and the obtained 3D coordinate point is Q_i . After that, reproject the 3D coordinate point back to the two image planes, denoted as $\hat{P}_j Q_i$, where $\hat{P}_1 = K_1 [I|0]$ and $\hat{P}_2 = K_2 [R|t]$. They are the projection matrix of the left and right cameras. The difference between the reprojection point and the original coordinate point is the reprojection error. The optimal solution of camera pose parameters can be obtained by minimizing this reprojection error. The solving equation of the BA method can be expressed as:

$$(\alpha_x, \alpha_y, \alpha_z, t_x, t_y, t_z)_{opt} = \arg \min \sum_{i=1}^n \sum_{j=1}^2 \left\| \hat{P}_j Q_i - q_{ij} \right\| \quad (4)$$

where $\alpha_x, \alpha_y, \alpha_z$ are the components of the rotation vector r , and t_x, t_y, t_z are the components of the translation vector t . Their relationship can be expressed by the following formula:

$$r = [\alpha_x \quad \alpha_y \quad \alpha_z]^T \quad (5)$$

$$t = [t_x \quad t_y \quad t_z]^T \quad (6)$$

The rotation vector r can be converted into a 3×3 rotation matrix R through Rodrigues transformation. The optimization method used here is the Levenberg-Marquardt algorithm, which has the advantages of easy implementation and fast convergence speed [22]. Through the BA method, the optimal camera pose parameters can be obtained.

Here are a few things to note. 1. The above theory is based on the ideal pinhole camera model without lens distortion. However, in actual application scenarios, lens distortion cannot be ignored. Therefore, before calculating the essential matrix and applying the BA method, it is necessary to correct the distortion of the coordinates of the corresponding point according to the distortion coefficient obtained by the calibration [13]. 2. The external parameters calculated by decomposing the essential matrix may have more than one set of solutions, and the redundant solutions can be eliminated by applying positive depth constraint [23]. The constraints for eliminating redundant solutions are as follows. The feature point in the space must be in front of the two cameras. Therefore, the point after 3D reconstruction should be positive in the z -axis direction. The sign of the translation vector

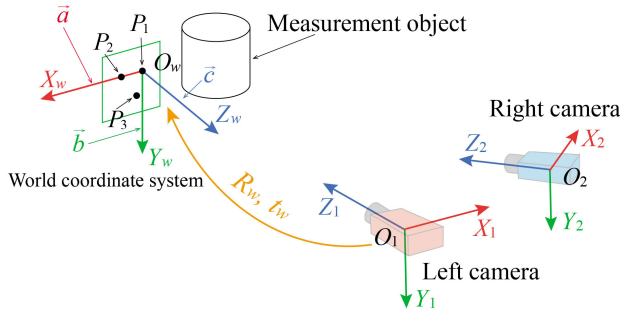


FIGURE 2. Schematic diagram of the three-point marking method to set the world coordinate system.

can be judged according to the position relationship of the cameras. 3. The translation vector calculated by the above method is the normalized results, where $\|t\| = 1$. This has no effect on the strain measurement of DIC. As long as there is a known size in the view, it can be restored to its true size. In this paper, the three marked points can be used as known dimensions in the view.

B. THREE-POINT MARKING METHOD FOR SETTING THE WORLD COORDINATE SYSTEM

Three points that are not collinear in space can define a plane. In the DIC measurement process, as long as there are three feature points in the view that have not been deformed, they can be set to the world coordinate system according to certain rules. The principle of the proposed three-point marking method is shown in Figure 2.

It is assumed that the three feature points $P_1, P_2,$ and P_3 which are not collinear have not changed during the entire test. In the DIC calculation, the 3D reconstruction of each frame of image is carried out in the left camera coordinate system. So, the 3D coordinates of the three points P_1, P_2, P_3 in each image frame in the left camera coordinate system can be obtained. Then set the world coordinate system $O_w - X_w Y_w Z_w$ according to the following rules. Let the unit vectors of the three directions of the three coordinate axes of the world coordinate system in the left camera coordinate system be $\vec{a}, \vec{b},$ and \vec{c} , respectively. Among them, \vec{a} is parallel to the vector $\vec{P_1 P_2}$. The vector \vec{b} can be calculated according to the vertical condition and coplanar constraint:

$$\vec{a} \cdot \vec{b} = 0, \tag{7}$$

$$\vec{b} = \varepsilon_1 \cdot \vec{a} + \varepsilon_2 \cdot \vec{P_1 P_3}, \tag{8}$$

where ε_1 and ε_2 are arbitrary real numbers. By specifying that the Y_1 axis component of \vec{b} is positive, a unique vector \vec{b} can be determined. The coordinate systems used in this paper are all right-handed coordinate systems, so $\vec{c} = \vec{a} \times \vec{b}$. After determining the direction vectors of the three coordinate axes of the world coordinate system in the left camera coordinate system, the rotation matrix R_w between the two coordinate systems can be obtained. The translation vector t_w between the world coordinate system and the left camera coordinate system can be directly obtained from the vector $\vec{O_1 P_1}$. The conversion formula for converting the 3D coordinates in the left camera coordinate system to the 3D coordinates in the

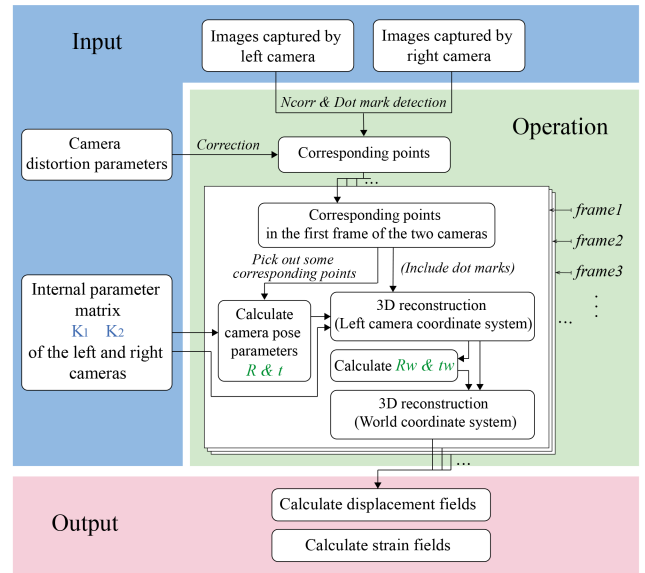


FIGURE 3. Overall stereo-DIC algorithm framework.

world coordinate system is as follows:

$$Q_{wi} = R_w [Q_i - t_w], \tag{9}$$

where Q_i is the 3D coordinate of a point in the left camera coordinate system, and Q_{wi} is its 3D coordinate in the world coordinate system.

C. STEREO-DIC OVERALL ALGORITHM FRAMEWORK

The overall stereo-DIC algorithm framework that integrates the camera pose self-estimation algorithm and the three-point marking method to set the world coordinate system is shown in Figure 3. The input of the entire system is images captured by stereo-camera system and the internal parameters of the cameras obtained by calibration. The output is the displacement field and strain field caused by the deformation of the measured object. The core of performing correlation calculations is the open source two-dimensional DIC software Ncorr [24]. Use Ncorr to perform correlation operations on all the captured images to obtain corresponding points. Next, calculate the camera pose in each frame. Calculate the camera pose parameters R and t at the moment when the stereo-camera system shoots each frame of image. And calculate the conversion parameters R_w and t_w between the left camera coordinate system and the world coordinate system at the time of each frame image shooting. Finally, the 3D coordinates of the 3D reconstruction of the measured object in the world coordinate system at the shooting time of each frame are obtained. According to the 3D coordinates of the measured object in the world coordinate system obtained at each shooting time, the displacement field and strain field of the measured object can be calculated.

III. SIMULATION

A. SIMULATION PRINCIPLE

The simulation image is generated by projecting the measured object onto the image plane of the binocular camera to verify the effect of the proposed method. The principle of

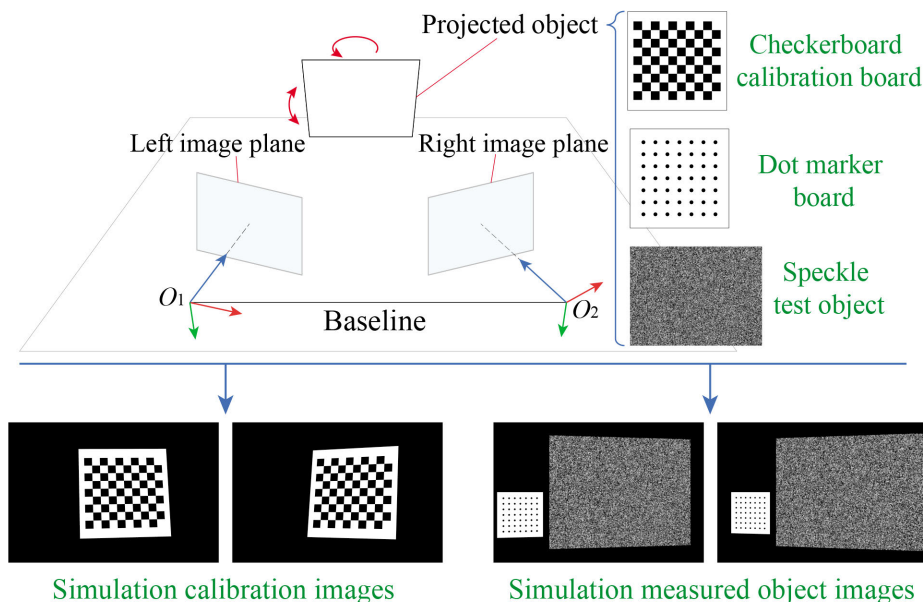


FIGURE 4. Simulation schematic.

simulation is shown in Figure 4. The initial baseline value of the stereo-camera system is set to 300 mm. The projected objects are checkerboard calibration board, speckle object and dot marker board. The size of the checkerboard calibration board image is 2048×2048 pixels², the number of squares is 9×10 , and the width of the squares is 180 pixels. Set the true size of the checkerboard to 150×150 mm². Here, a small circle calibration board is used as the dot marker board. The image size of the dot marker board is 2048×2048 pixels², the number of dots is 7×7 , the radius of the dots is 40 pixels, the pitch is 250 pixels, and the set true size is 70×70 mm². Although there are many dots on the dot marker board, only three of them that are not collinear are needed. The image size of the speckle test object is 3120×2340 pixels², the number of speckles is 10^6 , the characteristic size of the speckle is 6 pixels, and the true size is 240×180 mm². The detailed parameter settings of the stereo-camera system are shown in Table 1. The size of the generated simulation image is 3120×2340 pixels². At the beginning of the simulation experiment, first use the image of the checkerboard calibration board to generate simulated calibration images. Just like using a checkerboard calibration board to perform calibration in a real situation, photos of 15 different poses of the checkerboard are generated. An example is shown in Figure 4. The internal parameters of the left and right cameras obtained by using the checkerboard simulation images for calibration are shown in Table 2. C_x and C_y in the table represent the coordinates of the principal point of the camera. f_x , f_y represent focal length, here expressed in pixel values. γ represents the skew coefficient, and k_1 and k_2 represent the radial distortion coefficient of lens.

B. SELF-ESTIMATION OF CAMERA POSE

First, verify the effect of camera pose self-estimation based on speckle field. Use the above parameters to generate a pair

TABLE 1. Parameter setting of simulation stereo-camera system.

Simulation parameters	Left camera	Right camera
$C_x(pixel)$	1536	1536
$C_y(pixel)$	1024	1024
$f_x(pixel)$	6000	6000
$f_y(pixel)$	6000	6000
γ	0.02	0.02
k_1	0.5	0.5
k_2	-0.2	-0.2
$\alpha_x(radian)$	0	0
$\alpha_y(radian)$	0	0.4536
$\alpha_z(radian)$	0	0
$t_x(mm)$	0	292.3174
$t_y(mm)$	0	0
$t_z(mm)$	0	-67.4579

TABLE 2. Internal parameter obtained by calibration using simulation checkerboard images.

Parameters	Left camera	Right camera
$C_x(pixel)$	1535.39	1532.43
$C_y(pixel)$	1016.99	1022.49
$f_x(pixel)$	5997.44	5999.40
$f_y(pixel)$	5997.27	5999.30
γ	0.01	0.02
k_1	0.50	0.49
k_2	-0.07	-0.06

of binocular view images of the measured object. Then taking this pair of images and the internal parameters obtained by the above-mentioned simulation calibration as inputs, the operation is performed according to the flow of Figure 3. The region of interest (ROI) for correlation calculation is 1000×1200 pixels². The subset spacing is set to 9 pixels. Through correlation calculation, 12000 pairs of corresponding points are obtained. According to the correlation coefficient, 100 pairs of corresponding points were picked out to participate in the calculation of the camera pose. The calculated results are shown in Table 3.

TABLE 3. Calculation results of simulated checkerboard calibration and self-estimation of camera pose.

Parameters	Ground truths	Checkerboard calibration		Camera pose self-estimation	
		Measured values	Errors	Measured values	Errors
α_x (radian)	0.0000	0.0005	0.0005	-0.0000	-0.0000
α_y (radian)	0.4536	0.4539	0.0003	0.4533	-0.0003
α_z (radian)	0.0000	-0.0002	-0.0002	-0.0003	-0.0003
t_x (mm)	292.3174	292.0823	-0.2351	292.2564	-0.0610
t_y (mm)	0.0000	-0.0042	-0.0042	0.5760	0.5760
t_z (mm)	-67.4579	-67.3984	0.0595	-67.7322	-0.2743

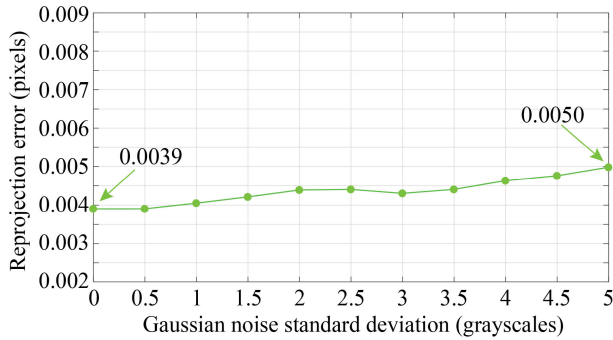


FIGURE 5. Relationship between Gaussian noise added to the calibration image and reprojection error (RMSE value).

In order to reflect the real scene, and in order to research the robustness of the camera pose self-estimation method based on speckle patterns, different degrees of Gaussian noise are added to the simulated images. The standard deviation of the added Gaussian noise ranges from 0 to 5 grayscale values, increasing in steps of 0.5 grayscale values. Reprojection error is a strict and widely accepted index for evaluating calibration accuracy [17]. Therefore, the reprojection error is used here to evaluate the accuracy of the camera pose calculation results.

The reprojection error here is the root mean square error (RMSE) between the points participating in the calculation and the points projected back. The calculation results are shown in Figure 5. In the absence of noise, the reprojection error is 0.0039 pixels. As the noise increases, the reprojection error rises slightly. When the standard deviation of the added Gaussian noise is 5 grayscale values, the reprojection error is 0.0050 pixels.

Next, the influence of the number of corresponding points that participated in the self-estimation calculation of the camera pose on the calculation result is studied. The ROI is still set to 1000×1200 pixels². The basis for screening the corresponding points is the correlation coefficient. In order to allow the selected points to be more evenly distributed in the entire ROI, a method of dividing the ROI into subregions is adopted. For example, if 100 pairs of corresponding points are selected, the ROI is evenly divided into 10×10 subregions, and the point with the best correlation coefficient in each subregion is selected. After the correlation calculation, according to the above rules, 100, 225, 400, 625, 1225, 1600, 2025, and 2500 pairs of corresponding points were selected.

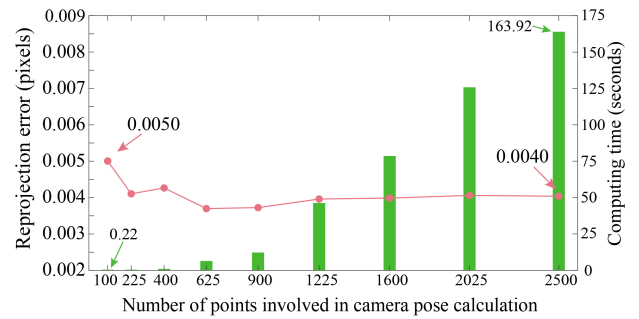


FIGURE 6. Relationship between the number of points and reprojection error (RMSE value) / computing time.

Use them to calculate the camera pose, respectively. The result is shown in Figure 6. It can be seen that as the number of points participating in the calculation increased, the reprojection error decreases slightly. After the corresponding point exceeds 625 pairs, the reprojection error becomes stable. However, as the number of points increases, the time required for calculation also increases. The CPU of the computer used in the calculation is i7-8565U, and the memory is 16 GB. The GPU used is NVIDIA MX250. The optimization algorithm is the Levenberg-Marquart algorithm. The specific parameter setting is as follows. The value of Function Tolerance is $1e-4$, and the value of Step Tolerance is $1e-4$. The maximum number of function evaluations allowed is set to $1e6$, and the maximum number of iterations allowed is set to 500. As the number of points increases, the calculation times used are 0.22s, 0.32s, 0.88s, 6.36s, 12.14s, 46.18s, 78.50s, 125.74s, and 163.92s, respectively.

C. SIMULATION OF STEREO-DIC WITH EXTERNAL PARAMETERS DISTURBED

Simulation images are used to verify that the proposed method can effectively deal with camera pose disturbance during the DIC measurement process. The schematic diagram of the simulation is shown in Figure 7. The simulation is divided into two scenarios: camera rotation and baseline length change. The measured object rotates around the axis of rotation 10 times, each time by 1° , and the binocular camera takes 11 frames of images. After each frame of images is taken, the cameras rotate by 0.1° , or the baseline changes by 1 mm. According to the conventional DIC method, 3D reconstruction is performed in the left camera coordinate system, and the results are shown in Figure 8(a) and Figure 10(a).

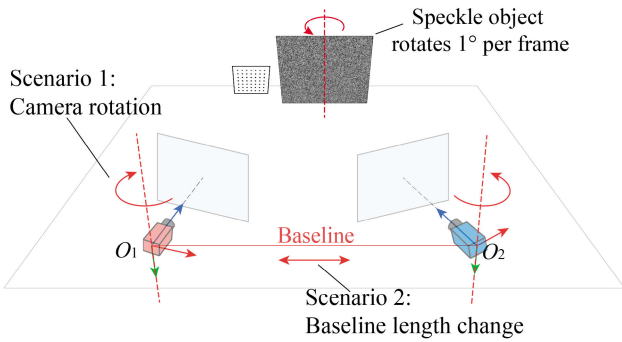


FIGURE 7. Schematic diagram of simulation of camera pose changes.

The results of 3D reconstruction in the world coordinate system determined by the three marked points are shown in Figure 8(b) and Figure 10(b). It can be seen from the figures that due to the change of the camera pose, the rotation axis of the measured object in the left camera coordinate system is significantly shifted. Even though the camera pose has changed, the 3D reconstruction results in the world coordinate system still reflect the correct rotation of the object.

In the simulation, the changes of external parameters are rotation and translation, respectively. Scenario 1 is the camera rotation. Every time an image is taken, the camera rotates by 0.1° . Scenario 2 is a change in the length of the baseline. Every time an image is taken, the baseline changes by 1 mm. The comparison between the measured value of the pose change calculated by the self-estimation method and the true value is shown in Figure 9 and Figure 11. The mean absolute error (MAE) of the measured value of the rotation angle is 3.68×10^{-4} rad, and the average relative error is 0.08%. The MAE of the measured value of the translation distance is 0.68mm (x-axis) and 0.54mm (z-axis), and the average relative error is 0.23% and 0.80% respectively.

IV. EXPERIMENT VERIFICATION

A. EXPERIMENTAL DEVICE

The experimental setup is the same as the simulation, and the experimental scenario is shown in Figure 12. The experiment device consists of a stereo-camera system, a turntable with a micrometer screw, a speckle test object, and a dot marker.

The stereo-camera system consists of two industrial cameras with a resolution of 3072×2048 . The focal length of the lens is 16 mm. The table diameter of the turntable is 82mm. The turntable is driven by a micrometer screw, and the resolution of the rotation angle is 2 minutes. The test object is a $240 \times 180 \text{ mm}^2$ rectangular flat plate with speckle pattern painted on it. A small circle calibration board with a size of $70 \times 70 \text{ mm}^2$ is used as a dot marker. The diameter of the dot is 3.75mm and the pitch is 7.5mm. The dot feature points will be used to reset the world coordinate system. Therefore, in order to reduce the error, it is recommended that the spacing between the selected feature points be as large as possible.

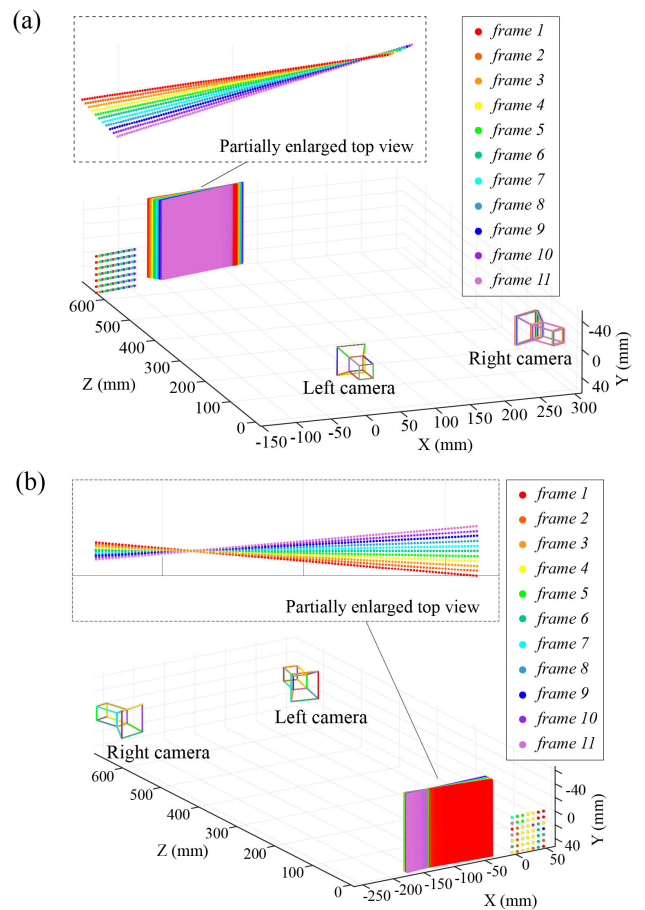


FIGURE 8. 3D reconstruction results under the camera rotation scenario: (a) in the left camera coordinate system; (b) in the world coordinate system determined by three points.

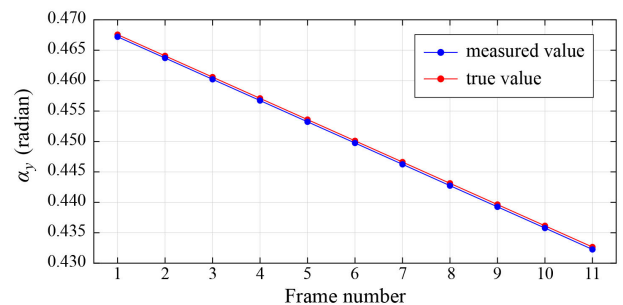


FIGURE 9. Comparison diagram of the measured and true values of the angle component in scenario 1.

B. COMPARISON OF DIC MEASUREMENT WITH OR WITHOUT CAMERA POSE DISTURBANCE

First, keep the stereo-camera system undisturbed, and the test object rotates 1° each time. Take 11 frames of images. Then perform DIC calculations. The ROI of DIC is $1000 \times 1200 \text{ pixels}^2$, as shown in Figure 13. Select three points that are not collinear on the dot marker board as marker points. After correlation calculations, 400 pairs of corresponding points were selected to participate in camera pose estimation. The result of 3D reconstruction is shown

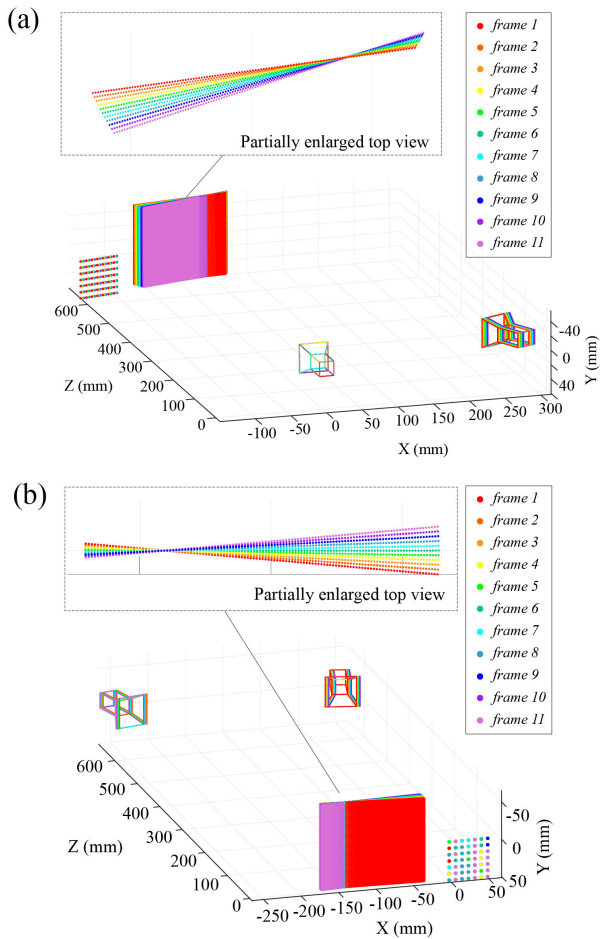


FIGURE 10. 3D reconstruction results with the baseline changed: (a) in the left camera coordinate system; (b) in the world coordinate system determined by three points.

in Figure 14(a). Next, reset the measured object and repeat the above process. Each time the measured object was rotated by 1° , and 11 frames of images were taken. However, this time in the process of capturing images, the stereo-camera system was randomly disturbed slightly. In the case that the camera pose was disturbed, the results of 3D reconstruction in the left camera coordinate system are shown in Figure 14(b). The results of 3D reconstruction in the world coordinate system determined by the three marked points are shown in Figure 14(c). It can be seen from Figure 14 that the rotation of the measured object is very uniform and tidy without the camera pose being disturbed. When the camera pose is disturbed, the reconstruction result of the measured object becomes messy. However, the propose method effectively overcomes the impact of the camera pose being disturbed.

According to the results of 3D reconstruction, calculate the rotation angle of the measured object in each case. The three cases in Figure 14 are respectively referred to as case 1, case 2, and case 3. Take the measured object of the first frame as the reference plane. In each subsequent frame, 10 position are randomly selected to calculate the angle of rotation of the measured object. The result is shown in Figure 15. It can be

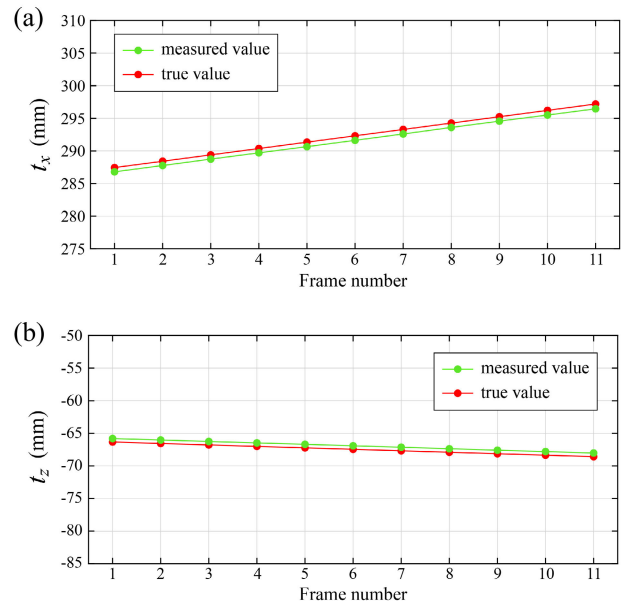


FIGURE 11. Comparison diagram of the measured and true values of the translation component in scenario 2: (a) x-axis component; (b) z-axis component.

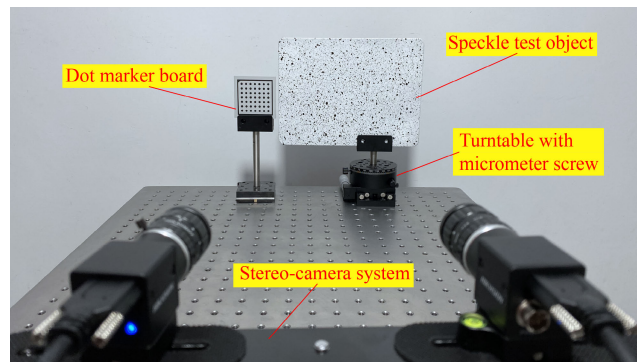


FIGURE 12. Experimental setup.

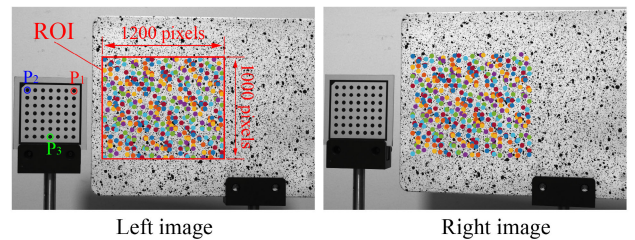


FIGURE 13. ROI of DIC and 400 pairs of corresponding points involved in camera pose self-estimation.

seen that the calculation results of case 1 and case 3 reflect the correct rotation angle, while the result of case 2 is obviously affected by the camera pose disturbance. The relative errors of case 1 and case 3 are shown in Figure 16. Their average relative errors are 0.67% and 0.73%, respectively. Therefore, the proposed method can effectively overcome the influence of external parameter disturbance. Even if the camera pose is disturbed, the measurement accuracy is not affected.

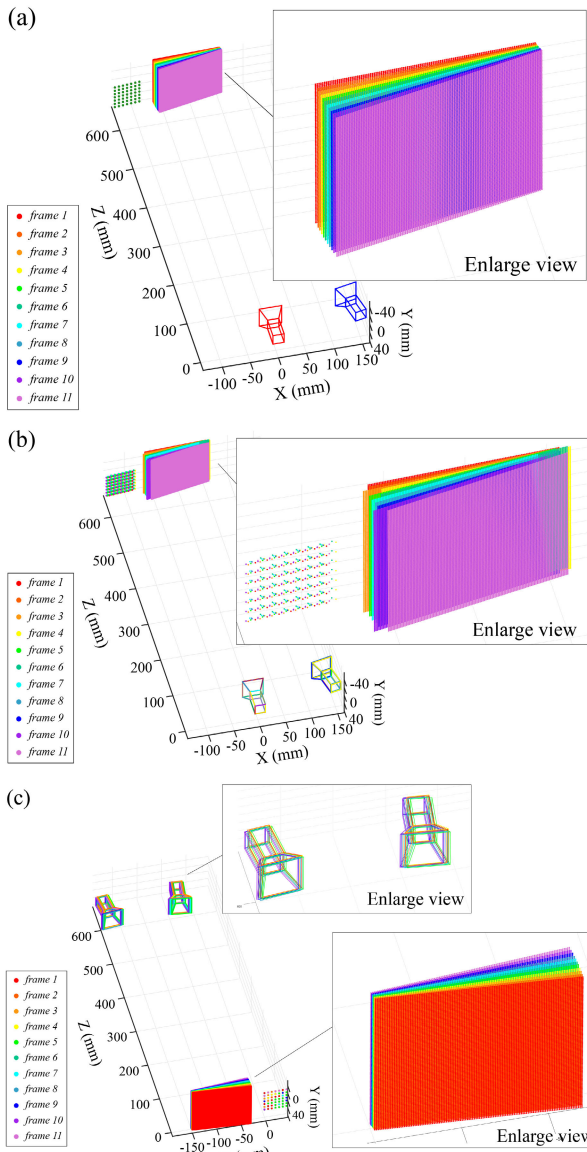


FIGURE 14. 3D reconstruction results: (a) the camera pose is not disturbed; (b) reconstruction results in the left camera coordinate system when the camera pose is disturbed; (c) reconstruction results in the world coordinate system when the camera pose is disturbed.

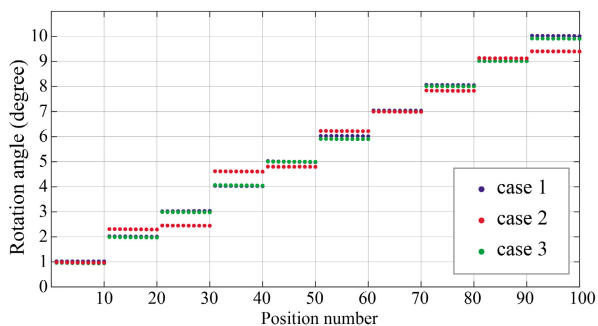


FIGURE 15. Calculation result of rotation angle.

C. NON-PLANAR OBJECT TEST

The proposed speckle-based camera pose self-estimation method is not only applicable to planar objects, but also

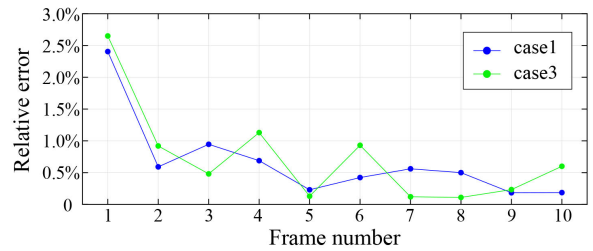


FIGURE 16. Relative error of case1 and case 3.

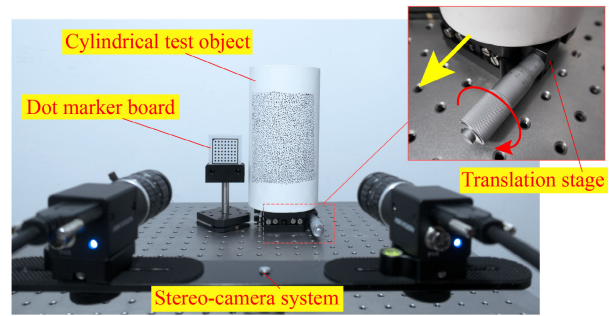


FIGURE 17. Experiment setup.

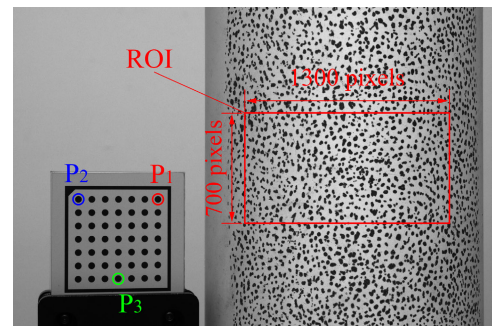


FIGURE 18. ROI and three marked points.

applicable to non-planar objects. Next, use a cylinder as the test object to verify the proposed method again. The experimental setup is shown in Figure 17. The object to be measured is a plaster cylinder with a height of 230 mm and a diameter of 110 mm. A large number of irregular spots were drawn on it with a gel pen. Below the cylinder is a precision translation stage. The resolution is 0.01 mm and the accuracy is 0.005 mm. Use 3M VHB double-sided tape to fix the cylinder on the translation stage.

Use a stereo-camera system to shoot the cylindrical object. Each time an image was taken, the object was moved forward by 0.5 mm. A total of 11 frames of images were taken, and the measured object moved forward by 5 mm. In the process of shooting, more severe disturbances were applied to the cameras. Arbitrarily change the camera angle, baseline, or rigidly translate the entire camera system. After the shooting is completed, the captured photos are processed according to the flow of Figure 3. The ROI for the correlation calculation and the three marked points as the world coordinate system are shown in Figure 18.

The results of 3D reconstruction in the world coordinate system are shown in Figure 19. It can be seen from the

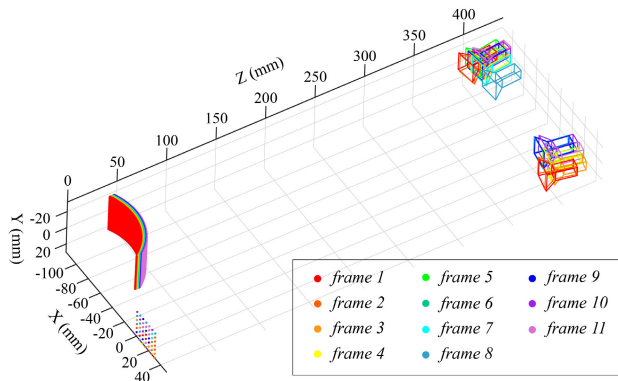


FIGURE 19. 3D reconstruction results and changes of camera pose.

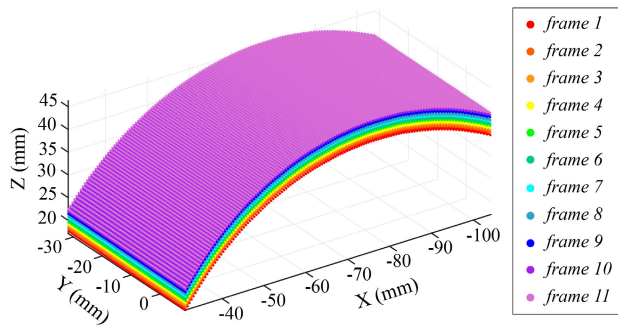


FIGURE 20. 3D reconstruction of the cylindrical shape.

figure that the result of the 3D reconstruction draws the shape of the cylinder well and reflects the process of its forward movement. The disturbance to the cameras is also reflected. Figure 20 shows the morphology and movement of the measured object.

V. CONCLUSION

In order to overcome the problem of external parameter disturbance in stereo-DIC, this paper proposes a three-point marking method for setting the world coordinate system and a camera pose self-estimation algorithm. Simulation and experiment prove that the proposed scheme can effectively overcome the influence of external parameter disturbance on DIC measurement. By adding varying noise to the simulated images, the robustness of the proposed camera pose estimation method is studied. The results show that as the noise increases, the reprojection error of the calculated camera pose parameters also increases, but the difference is not large. As the number of points involved in the calculation of camera pose increases, the reprojection error slightly decreases. After the number of points exceeds 625 points, the error tends to be stable. However, the required calculation time increases significantly with the increase of the number of points. The combination of the camera pose self-estimation method and the three-point marking method can overcome various changes of the camera pose including rotation, translation, and baseline change. The proposed method has no plane assumption and has good applicability. It effectively expands the application

scenarios of stereo-DIC and has good application potential in the fields of large-scale measurement, dynamic measurement, and structural health monitoring.

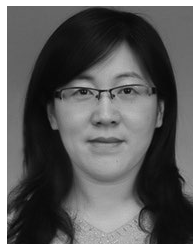
REFERENCES

- [1] B. Pan, "Digital image correlation for surface deformation measurement: Historical developments, recent advances and future goals," *Meas. Sci. Technol.*, vol. 29, no. 8, Jun. 2018, Art. no. 082001.
- [2] M. A. Sutton and F. Hild, "Recent advances and perspectives in digital image correlation," *Exp. Mech.*, vol. 55, no. 1, pp. 1–8, Jan. 2015.
- [3] Y. Gao, T. Cheng, Y. Su, X. Xu, Y. Zhang, and Q. Zhang, "High-efficiency and high-accuracy digital image correlation for three-dimensional measurement," *Opt. Lasers Eng.*, vol. 65, pp. 73–80, Feb. 2015.
- [4] Y. Shang, H. Zhang, H. Hou, Y. Ru, Y. Pei, S. Li, S. Gong, and H. Xu, "High temperature tensile behavior of a thin-walled ni based single-crystal superalloy with cooling hole: In-situ experiment and finite element calculation," *J. Alloys Compounds*, vol. 782, pp. 619–631, Apr. 2019.
- [5] L. Ngeljaratan and M. A. Moustafa, "Structural health monitoring and seismic response assessment of bridge structures using target-tracking digital image correlation," *Eng. Struct.*, vol. 213, Jun. 2020, Art. no. 110551.
- [6] B. Wisner, K. Mazur, and A. Kontsos, "The use of nondestructive evaluation methods in fatigue: A review," *Fatigue Fract. Eng. Mater. Struct.*, vol. 43, no. 5, pp. 859–878, May 2020.
- [7] Y. Katz and Z. Yosibash, "New insights on the proximal femur biomechanics using digital image correlation," *J. Biomech.*, vol. 101, Mar. 2020, Art. no. 109599.
- [8] L. Yu and B. Pan, "Single-camera high-speed stereo-digital image correlation for full-field vibration measurement," *Mech. Syst. Signal Process.*, vol. 94, pp. 374–383, Sep. 2017.
- [9] T. J. Bebernis and D. A. Ehrhardt, "High-speed 3D digital image correlation vibration measurement: Recent advancements and noted limitations," *Mech. Syst. Signal Process.*, vol. 86, pp. 35–48, Mar. 2017.
- [10] J. Li, B. Zhang, X. Kang, W. Xu, G. Yang, and L. Yang, "Single camera 3D digital image correlation using a polarized system," *Instrum. Exp. Techn.*, vol. 61, no. 1, pp. 99–105, Mar. 2018.
- [11] T. Siebert, "High-speed digital image correlation: Error estimations and applications," *Opt. Eng.*, vol. 46, no. 5, May 2007, Art. no. 051004.
- [12] Z. Chen, X. Zhang, and S. Fatikow, "3D robust digital image correlation for vibration measurement," *Appl. Opt.*, vol. 55, no. 7, pp. 1641–1648, Mar. 2016.
- [13] Z. Su, L. Lu, S. Dong, F. Yang, and X. He, "Auto-calibration and real-time external parameter correction for stereo digital image correlation," *Opt. Lasers Eng.*, vol. 121, pp. 46–53, Oct. 2019.
- [14] B. Pan, H. Xie, L. Yang, and Z. Wang, "Accurate measurement of satellite antenna surface using 3D digital image correlation technique," *Strain*, vol. 45, no. 2, pp. 194–200, Apr. 2009.
- [15] F. Q. Zhong, P. P. Indurkar, and C. G. Quan, "Three-dimensional digital image correlation with improved efficiency and accuracy," *Measurement*, vol. 128, pp. 23–33, Nov. 2018.
- [16] R. Liu, H. Zhang, M. Liu, X. Xia, and T. Hu, "Stereo cameras self-calibration based on SIFT," in *Proc. Int. Conf. Measuring Technol. Mechatronics Autom.*, Hunan, China, Apr. 2009, pp. 352–355, doi: 10.1109/ICMTMA.2009.338.
- [17] B. Chen and B. Pan, "Camera calibration using synthetic random speckle pattern and digital image correlation," *Opt. Lasers Eng.*, vol. 126, Mar. 2020, Art. no. 105919.
- [18] X. Shao, M. M. Eisa, Z. Chen, S. Dong, and X. He, "Self-calibration single-lens 3D video extensometer for high-accuracy and real-time strain measurement," *Opt. Express*, vol. 24, no. 26, pp. 30124–30138, Dec. 2016.
- [19] T. Luhmann, S. Robson, S. Kyle, and I. Harley, *Close Range Photogrammetry: Principles, Techniques and Applications*. Scotland, U.K.: Whittles Publishing, 2011, pp. 217–218.
- [20] D. Nister, "An efficient solution to the five-point relative pose problem," *IEEE Trans. Pattern Anal. Mach. Intell.*, vol. 26, no. 6, pp. 756–770, Jun. 2004.
- [21] M. Lourakis (2020). *Essential Matrix Estimation*. Accessed: Jun. 15, 2020. [Online]. Available: <https://www.mathworks.com/matlabcentral/fileexchange/67580-essential-matrix-estimation>

[22] M. Cao, L. Zheng, W. Jia, and X. Liu, "Fast incremental structure from motion based on parallel bundle adjustment," *J. Real-Time Image Process.*, to be published, doi: [10.1007/s11554-020-00970-3](https://doi.org/10.1007/s11554-020-00970-3).

[23] B. Guan, Y. Yu, A. Su, Y. Shang, and Q. Yu, "Self-calibration approach to stereo cameras with radial distortion based on epipolar constraint," *Appl. Opt.*, vol. 58, no. 31, pp. 8511–8521, Oct. 2019.

[24] J. Blaber, B. Adair, and A. Antoniou, "Ncorr: Open-source 2D digital image correlation MATLAB software," *Experim. Mech.*, vol. 55, no. 6, pp. 1105–1122, Mar. 2015.



HUI ZHANG (Member, IEEE) is currently an Associate Professor with the Precision Instruments and Optoelectronic Engineering School, Tianjin University. Her main research interests include intelligent nondestructive testing technology and MEMS ultrasonic transducer array and its applications in health monitoring.



CHANG MA received the B.S. degree from Tianjin University, in 2015, where he is currently pursuing the Ph.D. degree. His main research interests include digital image correlation and nondestructive testing.



HENGRUI CUI received the B.S. degree from the North University of China, in 2017. He is currently pursuing the Ph.D. degree with Tianjin University. His main research interests include digital image correlation and speckle metrology in residual stress measurement.



ZHOUMO ZENG (Member, IEEE) received the Ph.D. degree from Tianjin University, in 1993. He is currently a Professor and the Dean of the Precision Instruments and Optoelectronic Engineering School, Tianjin University. He is a member of the China Society of Optics and Optoelectronics Professional Committee, the Director of the China Microelectronics Society, and the Director of the Tianjin Microcontroller Society.



XIAOBO RUI received the B.S. degree from Tianjin University, in 2014, where he is currently pursuing the Ph.D. degree. His main research interests include piezoelectric energy harvesting and intelligent sensing technology.

...